Lasers Without Internal Heat Generation

Steven R. Bowman

***Abstract*—A new approach to the design of optically pumped solid-state lasers is proposed which permits lasing without detrimental heating of the laser medium. Very high average power lasers should be possible by balancing the radiated and absorbed power density at each point within the laser medium.**

***Index Terms*—Fluorescence, power lasers, solid lasers, thulium, ytterbium.**

I. Introduction

CONVENTIONAL solid-state lasers are exothermic. The processes of excitation and stimulated emission always result in heat generation within the lasing medium. This produces increased temperatures and stresses in the lasing medium which limit beam quality and average power. Over the last three decades, enormous effort has been devoted to increasing the power of laser systems. These efforts have concentrated on the developing techniques for effective cooling and limiting thermal beam distortions. Some of the more successful techniques have been the development of slab laser geometries, compensated resonator designs, and phase conjugation. Currently, solid-state lasers with moderate beam quality are available with average powers up to several hundred watts [1]–[3]. Increasing the average power further can be achieved only at the cost of substantially increased complexity or decreased beam quality. Thermal stress fracture ultimately limits the maximum average power for any solid-state laser material with the highest power laser near the 1-kW level.

This paper considers the problem of laser power scaling from a different approach, that of drastically reducing or eliminating the heat generated during the optical pumping and lasing process. It is proposed to use radiation cooling by anti-Stokes fluorescence within the laser medium to balance the heat generated by the Stokes shifted stimulated emission, the balance to be maintained through optical control of the laser and pump intensities. The result would be a radiation balanced laser device in which no excess heat is generated because the average quantum defect of the radiation process is adjusted to zero. If such a laser device can be realized, much higher average powers systems should be possible without many of the thermal and beam quality issues that limit conventional solid-state lasers.

The physical mechanism of radiation cooling by anti-Stokes fluorescence was originally proposed by Pringsheim in 1929 [4]. The phenomenon was first observed in 1981 using CO_2 gas [5]; however, fluorescence cooling of a solid has only recently been reported [6]. The cooling mechanism works because absorption of a photon can temporarily push an atom away from thermal equilibrium with its surroundings. If the atom then spontaneously emits after the thermal equilibrium has been reestablished, any frequency shift in the fluorescence results in a net heating or cooling of the material. Cooling effects of up to 2% of the absorbed power have been observed in ytterbium-doped ZBLANP glass. While this is a relatively inefficient cooling mechanism, it is comparable to the minimum heat generation required in low quantum defect lasers materials, like ytterbium glass. Finding the materials and conditions under which stimulated emission just offsets the effect of fluorescence cooling is the challenge of radiation-balanced operation.

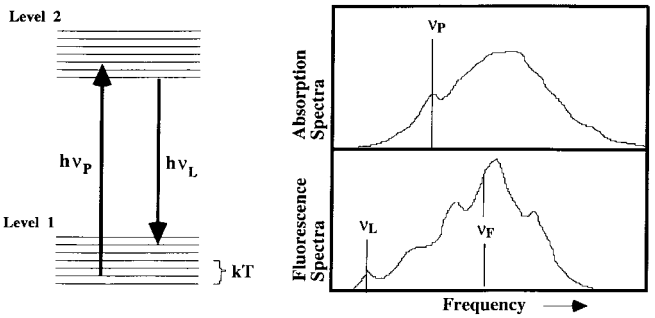

Fig. 1. A generic quasi-two-level energy diagram with the pump and lasing transitions. Absorption and fluorescence spectra showing the required ordering of the laser, pump, and fluorescence frequencies for radiation-balanced lasing.

This paper develops the basic concepts of radiation-balance lasing. A simple set of conditions for radiation-balance lasing are derived for the case of CW systems. Propagation conditions and some of the practical considerations are discussed. Finally, two specific laser materials, ytterbium at 1 μm and thulium at 2 μm, are modeled for radiation-balanced operation.

II. Radiation Balanced Lasers

In order to achieve a radiation-balanced laser system, it is necessary to properly select the laser material, operating wavelengths, and intensities. Consider a laser material which closely approximates an ideal quasi-two-level lasing system, as shown in Fig. 1. (Solid-state lasers of this type are often referred to in the literature as quasi-three-level systems. The term quasi-two-level is used here to emphasize that the quantum energy defect of these laser systems is only of the order kT.) Transitions between the upper and lower electronic levels are assumed to be purely radiative. This is an important

Manuscript received June 22, 1998; revised September 14, 1998. This work was supported by the Office of Naval Research.

The author is with the Laser Physics Branch, Naval Research Laboratory, Washington, DC 20375-5320 USA.

Publisher Item Identifier S 0018-9197(99)00209-2.

U.S. Government work not protected by U.S. copyright.

requirement for radiation balance. Deviations of real materials from the idealized system will be discussed in a later section. Labeling the number densities of atoms in the first and second energy levels as N_1 and N_2, the total density must satisfy

$$N_T = N_1 + N_2. \tag{1}$$

It is also a requirement that the upper and lower electronic levels are split into many closely spaced sublevels with a total splitting of order kT. Transitions between these sublevels are also assumed to be purely nonradiative. Atoms in either level can then exchange energy with the optical phonons of the solid host matrix. Since the energy gap between individual states is much less than kT, the exchange occurs on a picosecond time scale. For laser materials of interest here, the radiative lifetime of the upper level will be on the order of milliseconds, so atoms in both levels can be assumed to occupy a thermal distribution of the individual states. It is precisely this thermalization of the upper and lower levels that produces frequency-shifted fluorescence which allows for radiation balance.

In the laser material described above, spontaneous emission from the upper level will produce a broad fluorescence emission spectrum which partially overlaps the broad absorption spectrum of the lower level, as shown in Fig. 1. We define the average fluorescence frequency as

$$\nu_F = \frac{\sum_p \int_0^\infty \nu F_p d\nu}{\sum_p \int_0^\infty F_p d\nu} \tag{2}$$

where F_p is the fluorescence spectrum and the sum is over all possible polarizations. The position of ν_F with respect to the absorption spectra is a critical material characteristic for a potential radiation-balanced laser.

Now consider the interaction of the quasi-two-level system with a pump field at a frequency ν_P and a laser field at frequency ν_L, also shown in Fig. 1. System response to these fields can be described in terms of densities N_1 and N_2 by using Boltzmann occupation fractions to compute the population of the pertinent individual states. Assuming the individual states to be nondegenerate, the thermal occupation fractions associated with the absorption process at $h\nu_P = \varepsilon_{p2} - \varepsilon_{p1}$ will be given by

$$\mathcal{P}_1 = \frac{\exp\left[\frac{(-\varepsilon_{P1})}{\mathrm{kT}}\right]}{\sum_j^{\text{level 1}} \exp\left[\frac{(-\varepsilon_{1j})}{\mathrm{kT}}\right]}$$

and

$$\mathcal{P}_2 = \frac{\exp\left[\frac{(\varepsilon_2 - \varepsilon_{P2})}{\mathrm{kT}}\right]}{\sum_i^{\text{level 2}} \exp\left[\frac{(\varepsilon_2 - \varepsilon_{2i})}{\mathrm{kT}}\right]}. \tag{3}$$

The thermal fractions associated with the stimulated emission process at $h\nu_L = \varepsilon_{L2} - \varepsilon_{L1}$ will be given by

$$\mathcal{L}_1 = \frac{\exp\left[\frac{(-\varepsilon_{L1})}{\mathrm{kT}}\right]}{\sum_j^{\text{level 1}} \exp\left[\frac{(-\varepsilon_{1j})}{\mathrm{kT}}\right]}$$

and

$$\mathcal{L}_2 = \frac{\exp\left[\frac{(\varepsilon_2 - \varepsilon_{\mathbf{L}2})}{\mathrm{kT}}\right]}{\sum_i^{\text{level 2}} \exp\left[\frac{(\varepsilon_2 - \varepsilon_{2i})}{\mathrm{kT}}\right]}. \tag{4}$$

Here ε_2 is the energy of the lowest state in level two. The thermal fractions can be computed for any particular laser material by selecting the specific optical transitions and using the measured energy states. The time evolution of this system can be described in terms of a pump rate W_P, a stimulated emission rate W_L, and a fluorescence lifetime τ

$$\frac{\partial N_2}{\partial t} = W_P - W_L - \frac{N_2}{\tau}. \tag{5}$$

For simplicity, assume that overall system gain is small enough so that amplified spontaneous emission rates can be neglected. Conventional laser modeling would solve (5) along with propagation equations for the pump and laser fields. Applying the notation for the quasi-two-level system to (5) gives the following rate equation:

$$\frac{\partial N_2}{\partial t} = \frac{\sigma_P I_P}{h\nu_P}[\mathcal{P}_1 \cdot N_T - (\mathcal{P}_2 + \mathcal{P}_1) \cdot N_2] - \frac{\sigma_L I_L}{h\nu_L}[(\mathcal{L}_2 + \mathcal{L}_1) \cdot N_2 - \mathcal{L}_1 \cdot N_T] - \frac{N_2}{\tau} \tag{6}$$

where I and σ are the intensities and cross section for the pump and laser fields. For modeling the steady-state system, the time derivative of (6) would be set to zero.

Population inversion and laser gain are insured when W_L is positive. Absorption of the pump radiation requires that W_P be positive. Both conditions will occur whenever the fractional excited state density satisfies

$$\frac{\mathcal{P}_1}{(\mathcal{P}_2 + \mathcal{P}_1)} > \frac{N_2}{N_T} > \frac{\mathcal{L}_1}{(\mathcal{L}_2 + \mathcal{L}_1)}. \tag{7}$$

From the definitions of the thermal fractions $\mathcal{P}$ and $\mathcal{L}$, it follows that both population inversion and pump absorption can only be obtained when $\nu_P > \nu_L$, as expected.

For radiation-balanced lasing, we add the requirement that the time-averaged absorbed power density equals the radiated power density

$$h\nu_P \cdot \langle W_P \rangle = h\nu_L \cdot \langle W_L \rangle + h\nu_F \cdot \frac{\langle N_2 \rangle}{\tau}. \tag{8}$$

Combining this constraint with the time-averaged form of (5) gives the fundamental relation for a radiation balanced laser

$$\frac{\langle W_L \rangle}{(\nu_F - \nu_P)} = \frac{\langle N_2 \rangle}{(\nu_P - \nu_L)\tau} = \frac{\langle W_P \rangle}{(\nu_F - \nu_L)}. \tag{9}$$

For a radiation-balanced laser, both the pump absorption rate and stimulated emission rate must be restricted by the intrinsic spontaneous emission rate. When combined with the requirements for pump absorption and laser gain, (9) constrains the ordering of the transition frequencies, as illustrated in Fig. 1: $\nu_F > \nu_P > \nu_L$.

The requirement for radiation balance allows immediately for the solution of (6). Although time-dependent solutions are possible, for simplicity consider the case of steady-state pumping and laser emission. For CW radiation-balanced lasing, the upper level density and laser intensity can be shown to be

$$N_2 = \frac{\mathcal{P}_1 \cdot N_T}{(\mathcal{P}_1 + \mathcal{P}_2)} \cdot \left(\frac{I_P}{I_P + I_{P\text{sat}}} \right) \tag{10}$$

and

$$I_L = \frac{\mathcal{P}_1 \cdot (\mathcal{L}_1 + \mathcal{L}_2) \cdot I_P \cdot I_{L_{\text{sat}}}}{(\mathcal{P}_1\mathcal{L}_2 - \mathcal{P}_2\mathcal{L}_1) \cdot I_P - \mathcal{L}_1(\mathcal{P}_1 + \mathcal{P}_2) \cdot I_{P_{\text{sat}}}}. \tag{11}$$

Here $I_{P_{\text{sat}}}$ and $I_{L_{\text{sat}}}$ are saturation intensities for the pump and laser fields defined as

$$I_{P_{\text{sat}}} = \frac{h\nu_P}{\sigma_P \tau(\mathcal{P}_1 + \mathcal{P}_2)} \cdot \left(\frac{\nu_F - \nu_L}{\nu_P - \nu_L} \right)$$

and

$$I_{L_{\text{sat}}} = \frac{h\nu_L}{\sigma_L \tau(\mathcal{L}_1 + \mathcal{L}_2)} \cdot \left(\frac{\nu_F - \nu_P}{\nu_P - \nu_L} \right). \tag{12}$$

Equations (10)–(12) are the basic conditions for a CW radiation-balanced laser. Before going further, a few comments should be made about this solution. First, recognize (10) as the standard expression for saturated pump absorption with a modified definition of the saturation intensity. Note that the standard definition of the pump saturation intensity is modified by the ratio of frequency differences. From the required frequency ordering, it is clear that the new pump saturation intensity will always be larger than the standard definition. This reduction in saturation of the pump absorption is a simple consequence of the required rate of stimulated emission. The natural scale of the laser intensity $I_{L_{\text{sat}}}$ is also modified from the normal definition by a ratio of frequency differences. However, from its definition, the new laser saturation intensity can be either larger or smaller than the standard value depending on the selection of ν_P and ν_L.

The requirement that the system has gain at ν_L implies a minimum pump intensity. Also, pump saturation and radiation balance imply a minimum laser intensity. From (10) and (11), the minimum intensities required for radiation-balanced lasing are

$$I_{P_{\min}} = \left(\frac{\mathcal{L}_1 \cdot (\mathcal{P}_1 + \mathcal{P}_2)}{\mathcal{P}_1\mathcal{L}_2 - \mathcal{P}_2\mathcal{L}_1} \right) \cdot I_{P_{\text{sat}}}$$

and

$$I_{L_{\min}} = \left(\frac{\mathcal{P}_1 \cdot (\mathcal{L}_1 + \mathcal{L}_2)}{\mathcal{P}_1\mathcal{L}_2 - \mathcal{P}_2\mathcal{L}_1} \right) \cdot I_{L_{\text{sat}}}. \tag{13}$$

These minimum intensities are useful figures of merit in the selection of candidate materials and operating frequencies for a radiation-balanced laser.

The direct coupling between the laser and pump intensities given by (11) is a novel condition of radiation balance lasing. The laser intensity is required to maintain this relation with the pump intensity at each point in space. As a result, it is easy to show that the internal optical efficiency must be

$$\eta_o = \frac{\text{Stimulated emission power}}{\text{Absorbed pump power}} = \frac{(\nu_F - \nu_P) \cdot \nu_L}{(\nu_F - \nu_L) \cdot \nu_P}. \tag{14}$$

Note that the internal efficiency is independent of excitation level or any details of the optical system. The implications of maintaining radiation balance within a real laser system will be discussed in the next sections.

Before moving on to the details of proposed laser systems, it is interesting to consider the thermodynamic consistency of radiation-balanced lasing. Optically pumped solid-state lasers perform work by converting multimode and often broad-band pump beams into a single beam of narrow-line high-brightness radiation. The entropy flux of a CW laser beam is small but proportional to the number of cavity modes of the radiation [7]. As a result, the entropy flux of the laser medium produced by the pump and laser beams is small, but negative. In conventional lasers, the excess heat generated creates enough additional entropy to easily satisfy the second law of thermodynamics for the lasing medium [8]. However, when there is no heat generation, some other mechanism must be considered in order to satisfy the second law. For radiation-balanced lasers, the positive entropy flux is maintained through the disorder of the spontaneous emission. The spontaneous emission which is incoherent, broad-band, and omnidirectional fills all possible modes of the radiation field. The result is a large positive entropy flux from the laser medium which easily offsets the small negative flow of laser beam conversion. It is precisely this large entropy flux from spontaneous emission that makes radiation cooling by anti-Stokes fluorescence thermodynamically possible [9], [10].

III. Propagation Within a Radiation-Balanced Laser

So far, we have considered radiation balance only at a single point within the material. In this section, we consider the problem of maintaining the radiation balance as beams propagate through the laser material. It is not necessary to consider all possible laser geometries in order to reveal the fundamentals of the balanced propagation. For simplicity, first consider the case of a plane wave at the laser frequency propagating through a steady-state single-pass amplifier. The standard relation for laser gain applies

$$\frac{\partial I_L}{\partial z} = h\nu_L \cdot W_L = \sigma_L \cdot [(\mathcal{L}_2 + \mathcal{L}_1) \cdot N_2 - \mathcal{L}_1 \cdot N_T] \cdot I_L. \tag{15}$$

Now assume that this wave propagates in steady state radiation balance and solve for the pump intensity necessary to maintain the balance. The density N_2 can be eliminated from (15) using (9) and (10) to give

$$\frac{\partial I_L}{\partial z} = \frac{\alpha_L \cdot I_{L\text{sat}} \cdot I_L}{(I_L - I_{L\text{sat}})}. \tag{16}$$

Here the laser absorption coefficient is defined in the usual way, $\alpha_L = \sigma_L \mathcal{L}_1 \cdot N_T$. Notice that the requirement of radiation balance has modified the sign in the denominator from the normal expression for saturation gain in a homogeneous laser medium. Radiation balance automatically requires gain since

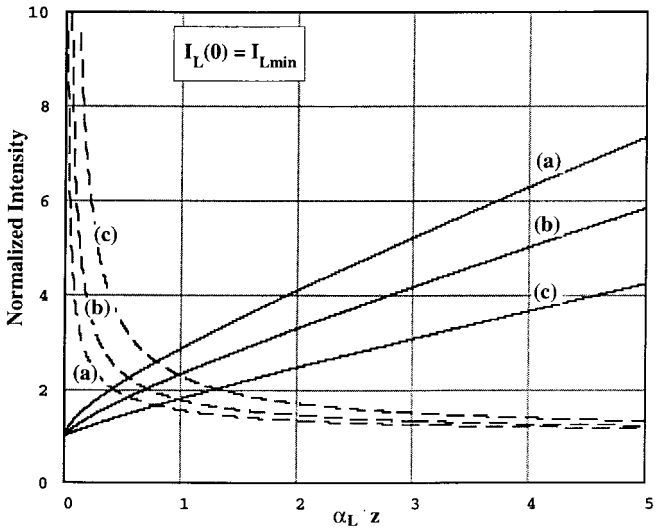

Fig. 2. The longitudinal intensity profiles within a radiation-balanced CW laser for which (a) $I_{L\min} = 1.1I_{L\text{sat}}$, (b) $I_{L\min} = 1.4I_{L\text{sat}}$, and (c) $I_{L\min} = 2.0I_{L\text{sat}}$. Both the laser intensities (solid lines) and the pump intensities (dashed lines) are normalized to their minimum allowed values as defined in (13). The laser intensities injected at $z = 0$ are set to the minimum value.

$I_L > I_{L_{\min}} > I_{L\text{sat}}$. Direct integration of (16) from 0 to z gives

$$\frac{I_L(0)}{I_L(z)} \cdot \exp\left[\frac{I_L(z) - I_L(0)}{I_{L_{\text{sat}}}}\right] = \exp[\alpha_L \cdot z]. \tag{17}$$

Therefore, a plane wave propagating in radiation balance must grow according to (17). To maintain balance for one-way propagation, the gain and pump intensity along the axis must be varied accordingly. The pump intensity profile that will produce the required gain can now be computed directly using (10) and (17). Fig. 2 plots the balanced intensities along the axis for the important case of minimal injected laser power, $I_L(z = 0) = I_{L_{\min}}$.

Unlike conventional lasers, gain in a radiation-balanced laser is determined solely by the injected laser intensity, temperature, and fundamental material parameters. Note that the growth in Fig. 2 is closer to linear than to exponential. For gain lengths of only a few absorption depths, the saturated single-pass gain $G \equiv I(z)/I(0)$ will be modest. Note that whenever $I_L(z) > 2 \cdot I_{L\min}$, the pump intensity varies slowly in the range $2 \cdot I_{P\min} > I_P > I_{P\min}$. As a result, $2 \cdot I_{L\text{sat}}$ may be a more practical lower limit for the injected laser intensity. Near the entrance face of the laser, the small-signal gain is limited by saturation of the pump with a maximum value of

$$g_{\max} = \frac{\alpha_L \cdot (\mathcal{P}_1\mathcal{L}_2 - \mathcal{P}_2\mathcal{L}_1)}{\mathcal{L}_1 \cdot (\mathcal{P}_1 + \mathcal{P}_2)}. \tag{18}$$

From this restriction on the small-signal gain, it is clear that the pump and laser frequencies must not be chosen too close together. The limited nature of the small-signal gain in these systems validates our earlier assumption neglecting amplified spontaneous emission rates.

The above results for plane wave propagation can also be applied for each ray within a finite collimated beam. As long as $I_L(z, r) > I_{L\min}$, each ray in the injected beam can be matched to a pump profile which will generate radiation-balanced gain. If the injected laser profile is center peaked, then the matching radial pump profile will have a minimum on-axis. In this case, the reduced on-axis gain will flatten the intensity profile of the amplified laser beam. Of course, extreme rays of the injected beam will have $I_L(z, r) < I_{L\min}$ and cannot be radiation balanced through stimulated emission. Absorbed pump power in this region of the laser material would result in radiation cooling and potential beam distortions. Fortunately, there are several approaches that could be used to maintain thermal neutrality in this region. The most obvious would be to introduce a small nonradiative loss in this region of the material to offset the effect of radiative cooling. This could be accomplished through spatially controlled irradiation or doping of the material. Alternatively, a slight blue shift to the pump spectra in this region would have a similar effect. Adverse edge effects could be further reduced by lowering the active ion density in this region to reduce pump absorption or by spatial filtering of the injected beam with super Gaussian optics to minimize the power content in the wings of the laser beam.

Although more constrained than conventional solid-state lasers, the conditions required for unidirectional steady-state radiation-balanced laser amplification should be possible using reasonable care in the design of a diode-pumped laser system. The details of such an optical design, however, must be determined through analysis of a specific laser system.

IV. Practical Considerations for Radiation-Balanced Lasers

The preceding analysis proves that radiation-balanced laser amplification is possible in principle. However, there are a number of important issues to be considered before such a system can be realized in practice. These issues can be roughly partitioned into two categories: the properties of suitable laser materials and special considerations in the optical design.

As mentioned earlier, in order for a laser material to be suitable for radiation-balanced operation, it must approximate an ideal quasi-two-level radiator. Even a relatively weak nonradiative decay mechanism can disrupt the radiation balance by converting some of the power density into heat. The nonradiative mechanisms most likely to adversely affect solid-state lasers are concentration quenching, impurity quenching, and multiphonon quenching of the active ions. Additionally, any nonradiative losses due to an impurity-induced absorption must be considered. Suitable materials must have total nonradiative loss rates less than a small fraction of the spontaneous emission rate

$$W_{NR} \ll \frac{1}{\tau} \cdot \frac{(\nu_F - \nu_P)}{\nu_P}. \tag{19}$$

For most potential laser materials, this implies that total nonradiative rates would be below 10 Hz. At these low rates, the radiation balance can be adjusted to compensate for the weak heat generation. Obtaining such laser materials with such low nonradiative rates will likely be one of the principle challenges of developing a practical device.

The requirement that the material have broad overlapping absorption and fluorescence spectra places additional constraints on potential laser materials. As mentioned earlier, the details of the spectral overlap are critical. The fluorescence spectra must be sufficiently broad to permit $h(\nu_f - \nu_L) \sim \mathrm{kT}$. There must also be a sufficiently strong absorption in the spectral region between ν_F and ν_L to allow effective coupling of the pump. The suitability of any particular material and transition frequencies can be judged by the values of the minimum intensities given in (13). Currently, the brightness of laser diode pump sources would restrict $I_{P\,\mathrm{min}}$ to values less than about 10 kW/cm^2.

One of the principle advantages of the radiation balance approach to laser design is a relaxation of the thermal constraints on the size of the laser medium. Without thermally induced birefringence, wave front distortion, and stress fracture, lasers powers can be scaled up by using larger apertures and longer gain paths. However, the process of radiation balance also places practical limits on the size of the laser medium. As discussed in the previous section, the laser medium should be optically thick for both the pump absorption and laser gain paths. However, to prevent radiation trapping of the fluorescence, the laser medium should be restricted to be optically thin in at least one dimension. This is desirable to maintain the radiative cooling and minimize the effects of nonradiative decay mechanisms. A practical estimate of the maximum allowed thickness can be computed from an average of the absorption spectra weighted with the fluorescence spectra

$$\alpha_F = \frac{\int_0^\infty \alpha_P \cdot F_P \, d\nu}{\int_0^\infty F_P \, d\nu}. \tag{20}$$

In this average, only the polarization with the strongest absorption is included. Keeping the laser medium thin in dimensions perpendicular to this emission axis will help minimize radiation trapping. Spontaneous emission escaping the laser medium can then be collected and removed by absorbing heat sinks. In this way, the heat removal process can be transferred away from the laser medium to materials and structures more amenable to high-power cooling. The increased overall system simplicity and efficiency that could be obtained with this type of radiative cooling has been an important motivation for this work.

The optical depth restrictions suggest consideration of edge-pumped slab or rod geometries. While end-pumped geometries should be possible, the additional complications of intensity profile matching and narrow-band dielectric coatings make that configuration less attractive. The unidirectional nature of the balanced amplification suggest that ring geometries may be required for resonator design. Two-pass power amplifiers may be possible using controlled laser beam divergence to maintain radiation balance.

The intensity constraints described in the previous section allow direct computation of the average power for radiation-balanced laser systems. For a crystal of length L, a beam area A, and an injected flat top laser beam with intensity of $2I_{L\mathrm{sat}}$, the average power will be

$$P_a = 2 \cdot I_{L\mathrm{sat}} \cdot (G - 1) \cdot A. \tag{21}$$

Here G is the single-pass saturated gain computed from (17). If the length of the gain medium is $2/\alpha_L$, then (17) gives $G = 2.45$. Using $2/\alpha_P$ and $1/\alpha_F$ as the approximate maximum transverse dimensions of the gain medium, a characteristic maximum power can be defined

$$P_{\max} = \frac{5.79 \cdot I_{L\mathrm{sat}}}{\alpha_F \cdot \alpha_P}. \tag{22}$$

The average power of radiation-balanced lasers scale with the optical depth of the material, unlike conventional solid-state lasers in which the average power scales with the thermal diffusion length. Further, (22) varies inversely as N_T^2 until the maximum available dimensions of the laser material are reached.

Of course, overall efficiency of the laser system will depend on a number of factors beyond the internal efficiency given by (14). Coupling of the pump source to the lasing medium is crucial and also depends on N_T. Weak absorptions will necessitate longer pump paths than in conventional systems. New fabrication techniques such as fusion bonding may be needed to obtain adequate crystal dimensions. As always, the selection of N_T will be important in the tradeoff between overall efficiency, power, and nonradiative losses.

The above analysis has considered only the case of steady-state radiation balance. It should also be possible to operate radiation balanced lasers in a high repetition rate Q-switched mode. As long as the averages described in (8) are computed for time scales short compared to the thermal diffusion times, radiation balance will be maintained. However, even in the CW lasing case, there are clearly transient and stability issues which need to be carefully considered for any specific systems.

V. Examples of Potential Radiation–Balanced Laser Systems

Using the considerations discussed above, a brief survey of well-characterized laser materials was conducted to identify the possible candidates for a prototype radiation-balanced system. The survey was restricted somewhat arbitrarily to ytterbium 1.0-μm and thulium 2.0-μm lasers in crystalline host materials. Candidate materials were primarily selected for the availability of complete spectral data.

The $^2F_{5/2} \Rightarrow {}^2F_{7/2}$ transition of ytterbium is one of the most promising candidates for a radiation-balanced laser. Of all the rare earths, Yb^{3+}, with its single excited state, most closely approaches the quasi-two-level ideal radiator. Nonradiative losses such as up conversion and multiphonon quenching are not an issue in this system. Efficient laser action near 1.03 μm has been demonstrated in several host materials [1], [3]. Unfortunately, the small number of sublevels in the upper and lower state combined with the low emission cross sections make finding an appropriate host for a radiation-balanced laser difficult. Yb : YAG, by far the most commonly studied material, was found to exhibit insufficient spectral overlap to be suitable for radiation-balanced lasing.

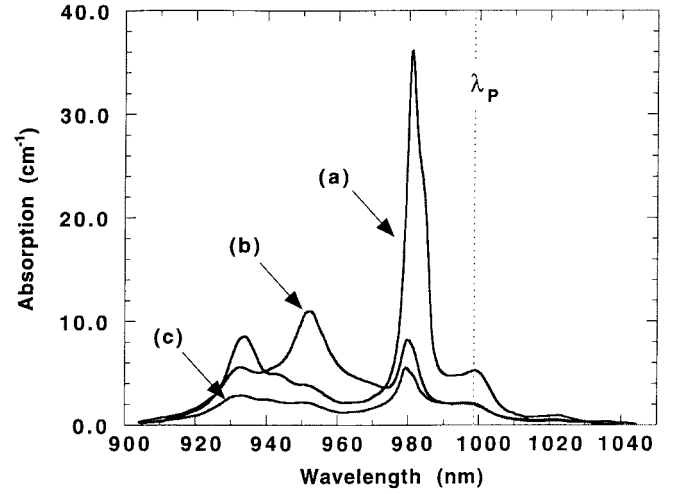

(a)

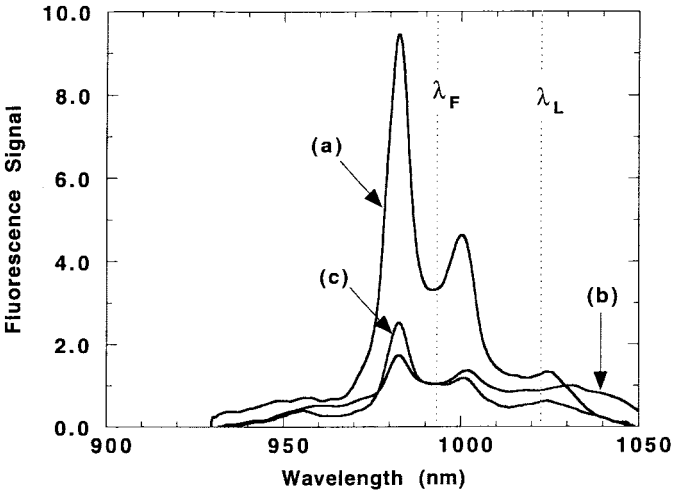

(b)

Fig. 3. (a) Room-temperature absorption and (b) fluorescence spectra from Yb:KYW with a doping density was 3×10^{20} cm^{-3}. Polarized spectra with electric fields parallel to the a, b, and c axes are as indicated. Positions of the average fluorescence, pump, and laser wavelengths are as shown. Spectral data were extracted from [11].

TABLE I
CRYSTALS DIMENSIONS $1\times1\times10$ cm^3 AS DESCRIBED IN TEXT

Material	Yb:KYW	Tm:YLF	
T	300	300	(K)
τ	0.6	15	(ms)
λ_L	1022.5	1913	(nm)
λ_P	998.2	1879	(nm)
λ_F	992.7	1821	(nm)
η_o	18.5	62.7	(%)
$\mathscr{L}_1$	0.085	0.042	
$\mathscr{L}_2$	0.75	0.36	
$\mathscr{P}_1$	0.27	0.068	
$\mathscr{P}_2$	0.75	0.36	
σ_L	1.8×10^{-20}	0.68×10^{-20}	(cm^2)
σ_P	6.6×10^{-20}	1.6×10^{-20}	(cm^2)
I_{Lsat}	5.0	4.5	(kW/cm^2)
I_{Lmin}	8.2	13.0	(kW/cm^2)
I_{Psat}	6.2	2.9	(kW/cm^2)
I_{Pmin}	3.9	5.5	(kW/cm^2)
N_T	3×10^{19}	1.4×10^{19}	(cm^{-3})
α_L	0.046 (b pol.)	0.039 (σ pol.)	(cm^{-1})
α_P	0.528 (a pol.)	0.150 (π pol.)	(cm^{-1})
α_F	1.02	0.54	(cm^{-1})
g_{max}	0.171	0.021	(cm^{-1})
P_{max}	54	326	(kW)
W_{NR}	$<< 3\times10^{19}$	$<< 3\times10^{19}$	(Hz-cm^{-3})
For crystals dimensions 1x1x10 cm as described in text			
G	1.86	1.14	
P_a	8.7	1.28	(kW)

The most promising candidate for a ytterbium radiation-balanced laser found in this survey was the high cross-section host material of potassium yttrium tungstate, $KY(WO_4)_2$. Spectroscopic and laser performance data for this material were recently reported [11]. This material is monoclinic and, when doped with 3×10^{20} Yb^{3+} ions/cm^3, exhibits the polarized absorption and fluorescence spectra, as shown in Fig. 3. At room temperature, the average fluorescence as defined in (2) occurs at 992.7 nm. Since the strongest fluorescence and absorption occurs for "a" axis polarized light, we choose a crystal thin in the "b" and "c" dimensions. Consider a laser at 1022.5 nm propagating along the "a" axis of the crystal and polarized parallel to the "b" axis. Further assume the material is transversely pumped at 998.2 nm with beams polarized parallel to the "a" axis. The relevant Boltzmann factors defined in (3) and (4) can be computed using the reported energy levels. The absorption and emission cross sections can then be computed directly from the absorption spectra using the reciprocity method. Even though the energy difference between the pump and laser is only 1.1 kT, the minimum intensities required for radiation-balanced lasing have very reasonable values in the range of several kW/cm^2. Assuming a doping level of 3×10^{19} cm^{-3} the single-pass saturated gain for 10 cm along the "a" axis would be 1.86. If the transverse dimensions of the beam are 1×1 cm^2, then the extracted laser power given by (21) should be 8.7 kW. The maximum power for this doping density would be 54 kW. In the absence of lasing, the fluorescence cooling rate would be only 0.55%. In the absence of spontaneous emission, the laser heat generation rate would be 2.4%. This choice of transitions gives the highest characteristic power but the optical efficiency as defined by (14) is only a modest 18.5%. The calculations for Yb:YKW are summarized in Table I. Upper limits on the nonradiative rates are well above multiphonon rates and should be obtainable in pure crystals. Alternative pump transitions with larger values of $(\nu_F - \nu_P)$ yield higher efficiencies but require somewhat higher intensities.

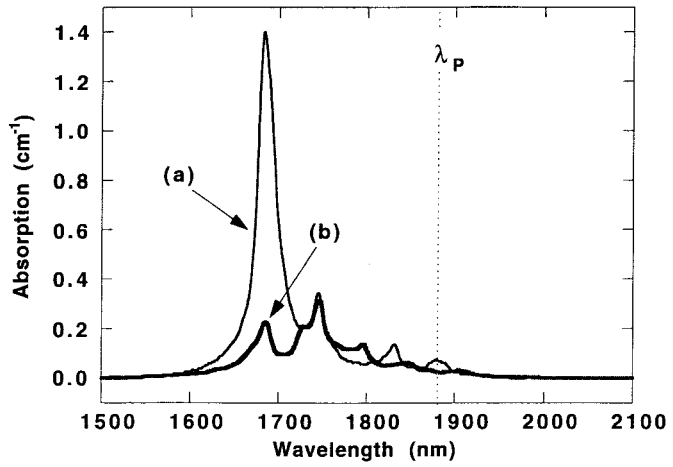

(a)

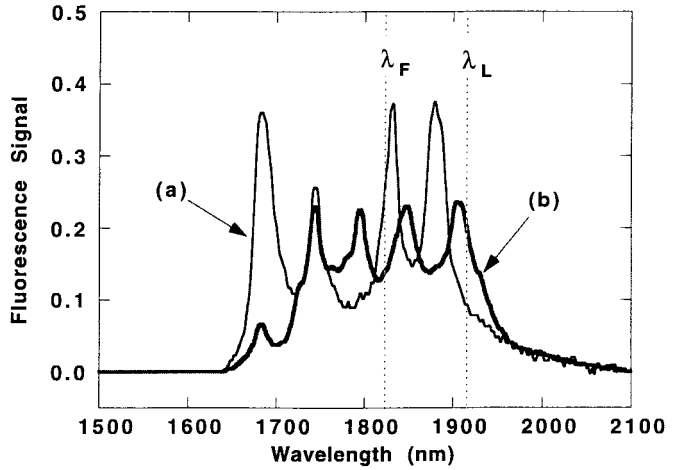

(b)

Fig. 4. (a) Room-temperature absorption and (b) fluorescence spectra from Tm^{3+} : YLF with a doping density of 7×1019 cm^{-3}: (a) π polarization and (b) σ polarization. The positions of the average fluorescence, pump, and laser wavelengths discussed in the text are shown. Spectral data were extracted from [14].

Another laser that could potentially operate in the radiation-balanced mode is the 2.0-μm thulium system. Although commonly pumped at 0.8 μm using concentration-induced cross relaxation, the thulium $^3F_4 \Rightarrow {}^3H_6$ transition could be directly pumped at 1.8 μm and operated as a quasi-two-level laser. The broad 2-μm emission features and numerous Stark components of this transition make Tm^{3+} an attractive system for radiation-balanced operation. As an example, consider Tm doped into the common host yttrium lithium fluoride (Tm : YLF). The spectroscopy of this material has been well characterized and the room-temperature spectra are shown in Fig. 4 [12]–[14]. Upconversion decay rates for the $^3F_4$ level can be estimated from previous measurements in higher concentrations crystals [15]–[17]. For 1% atomic Tm doping, the upconversion rate is projected to be below the maximum allowable nonradiative rate of 3×10^{19} Hz·cm^{-3}. Multiphonon quenching for 2-μm transitions is much more of an issue than at 1 μm. However, estimates of the rate are less certain due to the difficulty in determining the pure radiative decay lifetime. At room temperature, Tm : YLF energy gap projections for multiphonon decay rate are below 1 Hz [18], [19]. As shown in Fig. 4, the average fluorescence for Tm : YLF occurs at 1821 nm. Choosing a π-polarized pump at 1879 nm and a σ-polarized laser emission at 1913 nm gives an internal efficiency of 63%. Computing cross sections from the absorption spectra as before predicts minimum intensities of 5.5 kW/cm^2 for the pump and 13 kW/cm^2 for the laser. Reabsorption of the fluorescence is dominated by the π polarization with an average absorption length of 2 cm, assuming a thulium density of 1% atomic. If we again assume a crystal with dimensions $1\times1\times10$ cm^3, then the saturated single-pass gain would be 14% and the output power would be 1.3 kW. If larger aperture crystals were fabricated using a fusion-bonding process, the characteristic maximum average power for this material would be over 300 kW. This would be about 3000 times higher power than the current 100-W state-of-the-art in 2 μm thulium laser systems [1].

Rare-earth-doped glasses were excluded from this preliminary survey to avoid the complications of inhomogeneous broadening and impurity-induced nonradiative losses. However, reports of optical cooling in Yb : ZBLANP glass demonstrates that laser glasses should certainly be studied in the future [6]. Indeed, because of their potential for low scattering loss and large aperture, properly designed laser glasses may be the ideal choice for radiation-balanced laser systems. Future studies should also examine the erbium 1.5-μm and holmium 2.1-μm transitions. Both of these transitions have the potential to satisfy the radiation-balanced lasing requirements.

VI. Conclusions

A new mode of laser operation is proposed which should result in little or no heat generation within solid-state laser materials. The technique utilizes balanced spontaneous and stimulated emission within the laser medium. It is shown that this radiation balance can be maintained for single-pass amplification within collimated CW lasers. In the absence of thermal beam distortions or damage, average power scaling is shown to depend inversely on the optical depth of the solid-state laser material. Gain and overall efficiency constraints for the radiation-balanced laser system are also considered. Analysis of well-characterized Yb and Tm lasers indicates that scaling to the multi-kilowatt average power level with excellent beam quality is feasible. Laser systems of this scale and brightness would represent a major advance relative to the current state-of-the-art.

References

[1] S. A. Payne, R. J. Beach, C. Bibeau, C. A. Ebbers, M. A. Emanuel, E. C. Honea, C. D. Marshall, R. H. Page, K. I. Schaffers, J. A. Skidmore, S. B. Sutton, and W. Kurpke, "Diode arrays, crystals, and thermal management for solid-state lasers," *IEEE J. Select. Topics Quantum Electron.*, vol. 3, pp. 71–81, 1997.

[2] R. J. St. Pierre, D. W. Mordaunt, H. Injeyan, J. G. Berg, R. C. Hilyard, M. E. Weber, M. G. Wickham, G. M. Harpole, and R. Senn, "Diode array pumped kilowatt laser," *IEEE J. Select. Topics Quantum Electron.*, vol. 3, pp. 53–57, 1997.

[3] H. W. Bruesselbach, D. S. Sumida, R. A. Reeder, and R. W. Byren "Low-heat high-power scaling using InGaAs-diode-pumped Yb : YAG lasers," *IEEE J. Select. Topics Quantum Electron.*, vol. 3, pp. 105–116, 1997.

[4] P. Pringsheim, "Zwei Bemerkungen uber den Unterschied von Lumineszenzund Temperaturstrahlung," *Z. Phys.*, vol. 57, pp. 739–746, 1929.
[5] N. Djeu and W. T. Whitney, "Laser cooling by spontaneous anti-Stokes scattering," *Phys. Rev. Lett.*, vol. 46, pp. 236–239, 1981.
[6] R. I. Epstein, M. I. Buchwald, B. C. Edwards, T. R. Gosnell, and C. E. Mungan, "Observation of laser-induced fluorescent cooling of a solid," *Nature*, vol. 377, pp. 500–503, 1995.
[7] T. Graf and J. E. Balmer, "Laser beam quality, entropy and the limits of beam shaping," *Opt. Commun.*, vol. 131, pp. 77–83, 1996.
[8] T. Graf, J. E. Balmer, and H. P. Weber, "Entropy balance of optically pumped cw lasers," *Optics Comm.*, vol. 148, pp. 256–260, 1998.
[9] L. Landau, "On the thermodynamics of photoluminescence," *J. Phys.*, vol. 10, pp. 503–506, 1946.
[10] S. Yatsiv, *Advances in Quantum Electronics*, J. R. Singer, Ed. New York: Columbia Univ., 1961, pp. 200–213.
[11] N. V. Kuleshov, A. A. Lagatsky, A. V. Podlipensky, V. P. Mikhailov, E. Heumann, A. Diening, and G. Huber., "Highly efficient CW and pulsed lasing of Yb doped tungstates," in *Trends in Optics and Photonics, Vol. 10: Advanced Solid State Lasers*, C. R. Pollock and W. R. Bosenberg, Eds. Washington, DC: Opt. Soc. Amer., 1997, pp. 415–419.
[12] H. P. Jenssen, A. Linz, R. P. Leavitt, C. A. Morrison, and D. E. Wortman, "Analysis of the optical spectrum of Tm^{3+} in $LiYF_4$," *Phys. Rev. B*, vol. 11, pp. 92–101, 1975.
[13] M. Dulick, G. E. Faulkner, N. J. Cockroft, and D. C. Nguyen, "Spectroscopy and dynamics of upconversion in $Tm^{3+}:YLF_4$," *J. Lumin.*, vols. 48/49, pp. 517–521, 1991.
[14] B. M. Walsh, N. P. Barnes, and B. Di Bartolo, "Branching ratios, cross sections, and radiative lifetimes of rare earth ions in solids: Applications to Tm^{3+} and Ho^{3+} ion in $LiYF_4$," *J. Appl. Phys.*, vol. 83, pp. 2772–2787, 1998.
[15] G. Armagan, A. M. Bouncristiani, A. T. Inge, and B. Di Bartolo, "Comparison of spectroscopic properties of Tm and Ho in YAG and YLF crystals," in *OSA Proc. Advanced Solid-State Lasers*, G. Dube and L. Chase, Eds., 1991, vol. 10, pp. 222–226.
[16] S. R. Bowman, G. J. Quarles, and B. J. Feldman, "Upconversion losses in flashlamp-pumped Cr,Tm : YAG," in *OSA Proc. Advanced Solid-State Lasers*, L. L. Chase and A. A. Pinto, Eds., 1992, vol. 13, pp. 169–173.
[17] S. R. Bowman, J. E. Tucker, and S. Kirkpatrick, "Progress in the modeling of migration limited energy transfer in upconverting laser materials," in *Trends in Optics and Photonics, Vol. 19: Advanced Solid State Lasers*, W. R. Bosenberg and M. M. Fejer, Eds. Washington DC: Opt. Soc. Amer., 1998.
[18] C. Bibeau, S. A. Payne, and H. T. Powell, "Direct measurements of the terminal laser level in neodymium-doped crystals and glasses," *J. Opt. Soc. Amer.*, vol. B-12, pp. 1981–1992, 1995.
[19] T. T. Basiev, Y. V. Orlovskii, K. K. Pukhov, V. B. Sigachev, M. E. Doroshenko, and I. N. Vorob'ev, "Multiphonon relaxation rates measurements and theoretical calculations in the frame of nonlinear and non-Coulomb model of a rare-earth ion-ligand interaction," *J. Lumin.*, vol. 68, pp. 241–253, 1996.

Steven R. Bowman was born in Hickory, NC, in February 1956. He received the B.Sc. degree in physics from North Carolina State University, Raleigh, in 1978 and the M.Sc. and Ph.D. degrees in physics from the University of Maryland, College Park, in 1980 and 1986, respectively. His thesis research involved the design and testing of a high-precision lunar laser ranging facility.

He continued work in the areas of single-photon silicon detectors, high-power laser amplifiers, and precise time transfer as a Post-Doctoral Research Associate before joining the Naval Research Laboratory (NRL), Washington, DC, in 1987. Within the Laser Physics Branch of the NRL, he has worked on undersea laser communications, infrared optical countermeasures, mid-infrared solid- state laser materials, multiple-quantum-well optical modulators, and photorefractive devices.